Experimental determination of dispersion relationship of polyamide thin beams

Jelena Tomić[1*], Vladimir Sinđelić[1], Aleksandar Nikolić[1], Nebojša Bogojević[1]
[1]Faculty of Mechanical and Civil Engineering, University of Kragujevac, Kraljevo (Serbia)

Due to its superior mechanical properties, polyamide represents the most frequently used polymer material for additive manufacturing of automotive and aerospace components. With the perspectives of future use for on-site production in space, the field of application is extending to larger structures, raising interest for dynamic behavior of polyamide structures. The paper presents experimental study of dynamic response of thin beams made of three different types of polyamide: polyamide PA6, composite polyamide PA6 with 30% of glass fibers and polyamide PA12 obtained by selective laser sintering of polyamide powder PA2200. The results show that the dynamic response of polyamide beams is similar to metal beams.

Keywords: Polyamide, Additive manufacturing, Mechanical waves, Dispersion relationship

1. INTRODUCTION

The global demands for increasing energy efficiency through reduction in weight of motor vehicles and aircrafts and, consequently, reduction of energy consumption lead to increased use of polymers for industrial production [1]. In the past few years, the emergence of new types of polymers with different spectrum of mechanical and thermal characteristics resulted in a significant increase of polymer applications in all spheres of industry production and manufacturing. The application of modern tools for analysis of polymers impact on the environment and decision support for the manufacturing process, such as eco-efficiency assessment model (EEAM), life cycle assessment (LCA) and life cycle cost analysis (LCCA), has shown that the carbon footprint of manufacturing and environmental pollution can be notably reduced [2]. Furthermore, increased attention must be paid to the proper end-of-life disposal of parts made of polymers.

In addition to standard polymers, nowadays the interest for the application of biodegradable polymers in the industrial production has been increasing. Several studies have been conducted in order to determine if bio-polyamides as well as PLA (polylactic acid) may replace thermoplastics reinforced by natural fibers that are mainly used in the automotive industry [3].

The aerospace industry usually uses composites - a combination of two or more materials with different physical or chemical properties designed to have specific characteristics, such as added strength, efficiency or durability. With the aim of improving the mechanical properties of parts, composite material most often represents a combination of basic plastics such as polyamide, polypropylene, polyester and carbon fibers [4].

According to the latest analyzes, the automotive industry uses approximately 130 kg of different plastics for the production of one average middle-class passenger vehicle. During the exploitation, the polymer parts embedded in different types of systems are exposed to both mechanical loads and thermal influences.

Since the polyamide usually represents the basic polymer mass for the technical applications, transmission of vibrations through this material is the subject of study presented in the scope of this paper.

Polyamide (Nylon) is any polymer in which the repeating units in the molecular chain are linked by amide bonds. They are classified into various categories depending on the arrangement and chemical nature of monomers. Nowadays, imperative types of polyamides for technical application are PA6, PA6.6, PA 11, PA 12. Their properties, manufacture, processing and use are covered in the scope of paper [5].

With the development of new production processes, in addition to casting and injection molding, polyamide parts can also be made with additive manufacturing (AM). Due to main advantages of AM technology, such as material costs and waste reduction, production speed and efficiency, as well as the possibility of topology optimization, the aerospace became an early adopter of additive manufacturing. In aerospace industry, these manufacturing processes often use polyamide as a basic polymer for parts production.

Due to the difference in the structure of parts produced by conventional methods of manufacturing and parts produced by AM technology, this paper presents a comparative analysis of dispersion relationships of polyamide beam produced by AM (selective laser sintering) and polyamide beams produced by cutting the extruded plate.

2. DISPERSION RELATIONSHIP

Dispersion relationship (abbreviated as "DR" in the following text) expresses the relation between the wavenumber of a wave k and its angular frequency ω. Since it enables calculation of the phase and group velocities of the wave, the DR represents an important tool for wave propagation studies.

Thin beams represent the most convenient object for experimental determination of dispersion relationship. Depending on location and direction of the excitation, different types of mechanical waves may propagate through beams, such as longitudinal compression waves or torsional waves. The simplest mechanical waves for excitation and detection are flexural waves, which have

*Corresponding author: Jelena Tomić, Dositejeva 19, Kraljevo, tomic.j@mfkv.kg.ac.rs

parabolic form of dispersion relationship **Error! Reference source not found.**:

$$\omega = \sqrt{\frac{EI}{\rho A}} k^2 \quad (1)$$

In the equation (1), ρ stands for density, E represents Young's modulus of the beam material, I is the area moment of inertia, while A represents the area of the cross-section of the beam.

According to the Euler-Bernoulli beam theory for flexural waves in a free-free elastic beam [7], resonances occur when the wavenumber of wave k_m is equal to $(2m+1)\cdot k_0$, where $k_0=\pi/(2L)$, while L [m] represents the length of the beam's longest dimension. Resonant frequencies can be expressed with $f_m = (2m+1)^2 \cdot f_0$ with $f_0 = k_0^2 \cdot (EI)^{1/2}/(\rho A)^{1/2}/(2\pi)$.

2.1. Experimental determination of the DR

Experimental determination of dispersion relationship consists in measurement of the response (usually acceleration) to an excitation (usually impulse or harmonic) in multiple points along the beam. The responses at these points at a particular excitation frequency f are then used to construct wavefields with wavenumbers that have minimal deviation from the measured responses. There are several methods for wavefield construction and they differ in accuracy, mathematical complexity and range of applicability. The method that is the subject of this paper, so-called correlation method [8], uses a simple form of the wavefield and the sequential search of the wavenumber space in order to find the wavenumber value that provides maximum of correlation between the wavefield and measured response.

In its simplest one-dimensional form, which is used to study the waves propagating along a beam, the correlation method for experimental determination of DR (in further text just *"correlation method"*) uses test wavefields constructed on the basis of harmonic progressive waves with angular frequency ω and different test wavenumbers k_t. When the wave propagating along the beam is a progressive harmonic wave with wavenumber k, then the correlation between the wavefield of the wave and the test wavefield

$$\underline{W}_\omega(k_t) = \int_{-\infty}^{\infty} \underline{w}(x,\omega)\underline{w}_t{}^*(x,\omega)\,dx \quad (2)$$

will have the highest value when $k_t = k$. In the expression (2), x-axis is adopted as the direction of the wave propagation, $\underline{w}(x,\omega)$ and $\underline{w}_t(x,\omega)$ represent complex amplitudes of the progressive harmonic wave with wavenumber k and the constructed wavefield with the wavenumber k_t, respectively. In order to determine the DR of a wave in a frequency range $f_{min}<f<f_{max}$, the correlation method scans the wavenumber space in the range $k_{min}<k_t<k_{max}$ for each of the frequencies f, and assumes that the value of k_t that leads to the highest value of the correlation between the wavefield of the wave and the test wavefield is equal to the wavenumber that corresponds to the frequency f, denoted as $k(f)$.

Due to the discrete nature of input data (amplitudes of accelerances $\underline{w}(x_l,\omega) = \underline{w}_{l\omega}$ measured in L measurement points x_l, l=1,2,…,L, along the beam), the correlation (2) may be expressed as the following *correlation function* Y_ω:

$$Y_\omega(k_t) = \left|\sum_{l=1}^{L} \underline{w}_{l\omega} \exp(-ik_t x_l)\Delta x_l\right| \quad (3)$$

The scanning of the wavenumber space in the range $k_t^{min}<k_t<k_t^{max}$ consists in calculation of Y_ω values using equation (3) in a sufficiently large, but still finite number of points within the wavenumber range $k_t^{(j)}$ (j = 1,2,…, J). In the following text, the obtained array of points $Y_\omega^{(j)} = Y_\omega(k_t^{(j)})$ (j = 1,2, …, J) will be called "*the correlation array"*. The test wavenumber k_t that corresponds to the largest member of the correlation array is assumed to be the wavenumber that corresponds to the frequency f.

The implementation of the correlation method meets the challenges caused by a) the finite number of wavenumber test points; b) the finite number of measurement points.

The finite number of wavenumber test points may lead to omission of the actual wavenumber value that maximizes the correlation function, which results in misidentification of the wavenumber that corresponds to a frequency f.

On the other hand, due to the finite number of measurement points, for any wavenumber value k_t, there is an infinite number of wavenumbers $k_t' \neq k_t$ such that for each measurement point x_l holds:

$$\exp(-ik_t' x_l) = \exp(-ik_t x_l) \quad (l = 1,2,...,L), \quad (5)$$

As a consequence, there may be several local maxima with the same correlation function value within the wavenumber range $k_t^{min}<k_t<k_t^{max}$.

In the case of equidistant measurement points the equality (4) is satisfied for each measurement point if k_t'-$k_t = z(2\pi/d)$, where z is an integer. Therefore, within the wavenumber range $k_t^{min}<k_t<k_t^{max}$, the number of equal local maxima of the correlation function is $(k_t^{max}-k_t^{min})d/2\pi$. Direct application of the correlation method is thus reduced to the wavenumber range $-\pi/d<k_t<+\pi/d$, which is known as the first Brillouin zone (abbreviated as BZ). In the case of non-equidistant measurement points, the system of equations (4) still has an infinite number of solutions and the average difference between the solutions is close to $(2\pi/d)$, where d is the average distance between the measurement points **Error! Reference source not found.**.

The restriction of the wavenumbers range to the first BZ reduces the frequency range for the experimental determination of the DR to

$$f < f_{BZ} = \frac{\pi}{2d^2}\sqrt{\frac{EI}{\rho A}}. \quad (6)$$

In order to extend the frequency range for experimental determination of dispersion relationship of flexural waves in beams, artificial neural network (ANN) approach presented in the paper [10] has been used. A recurrent neural network (Fig. 1) is developed as a sequence prediction tool for estimation of the wavenumber corresponding to a frequency f using the wavenumbers of the previously determined points of the dispersion relationship. By implementing the sliding window technique, wavenumber values of the five previous DR points are used as neural network input data, while the difference Δk between two the current and the previous wavenumber values represents the target value at the network output layer. Developed neural network contains one hidden layer with five nodes and one output layer

containing one node. Bipolar sigmoid function and linear function are used as transfer functions of the hidden layer and the output layer, respectively.

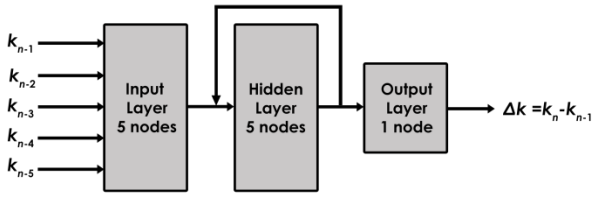

Figure 1: ANN network architecture

In order to define a neural network training data set, the straightforward correlation method has been applied for determination of the DR in a frequency range $f<f_{BZ}/2$. Resulted sequence of the wavenumbers has been used for the neural network training process.

For each frequency $f_n>f_{BZ}/2$, the wavenumber value is determined using the following steps:

- by using the wavenumbers of five previous points of dispersion relationship as neural network inputs, the wavenumber value k_{est} corresponding to frequency f_n is estimated by adding the output of developed ANN to the wavenumber of previous DR point
- the correlation array $Y_\omega^{(j)}$ (j=1,2,…,J) is calculated using the equation (3) and $\omega = 2\pi \cdot f_n$ for all test wavenumber points $k_t^{(j)}$ (j = 1, 2, …, J);
- after finding the local maxima in the obtained correlation array, the candidate array is created by selecting the wavenumbers corresponding to the local maxima such that relative difference between their correlation value and maximal correlation value is smaller than predefined value ε_Y;
- the element of the candidate array closest to the k_{est} value is selected as the final candidate k_{final} and its proximity rate is calculated by applying equation:

$$r(k_{final}) = \frac{|k_{final} - k_{est}|}{k_{est}}, \qquad (7)$$

- if the proximity ratio of the final candidate is lower than the proximity limit ε_k, then the final candidate k_{final} is accepted as the wavenumber corresponding to the frequency f_n; However, if the proximity ratio of the final candidate is higher than the proximity limit, the value k_{est} is accepted as the wavenumber corresponding to the frequency f_n

3. EXPERIMENT

For the purpose of experimental determination of dispersion relationship of mechanical waves propagating through polyamide thin beans, series of subsequent measurements of time history of acceleration $a_x(t)$ at a single point of a beam excited by impact hammer have been conducted.

3.1. Measurement objects

The experiment has been carried out on the following beams:

- polyamide beam produced by cutting from the plate (PA6 in the following text);
- glass filled polyamide beam produced by cutting from the plate (PA6GF in the following text);
- polyamide beam produced by selective laser sintering (PA3D in the following text);

Characteristics of the measurement objects are given in the Table 1.

Table 1: Properties of the measurement objects

beam	Length [cm]	Width [cm]	Height [cm]	E [GPa]	ρ [g/cm^3]
PA6	104	1.5	1	2.9	1.13
PA6GF	63.8	2.3	2	6	1.49
PA3D	30	1	1	1.65	8.67

With the aim to emulate a beam with free ends, the end parts of the beams were resting on soft sponges.

3.2. Excitation

The vibrations were excited by the impact hammer B&K 8204 with sensitivity 30.89 mV/N and the bandwidth up to 10 kHz. The excitation was measured by the B&K Pulse system with CCLD input with range ±10V. The force measurement range was around 300 N.

Automatic double-hit detection was not provided. In order to discard the double-hits, each excitation hit was monitored by inspecting the time history of impacting force F(t).

The beam was hit at the area 0-1 cm from the beam's beginning. In order to reduce excessive accelerations that prevented recording by the data acquisition software, the hitting area was covered by a piece of scotch-tape which provided a bit of dampening to the hit, but also reduced the bandwidth to around 6 kHz. The maximal impact force was in the range 10-25 N.

3.3. Response

The accelerometer B&K 4507Bx with sensitivity 10.055 mV/ms^{-2} and B&K Pulse system with CCLD input with range ±10V were used for measuring the response. Acceleration measurement range was around ±1000 m/s^2.

3.4. Experimental procedure

For each of the beams, the measurements of acceleration were carried out ten times for each of the measurement points. Time histories of excitation force and acceleration were recorded during each of the measurements. After each of the measurements, the data acquisition software calculated power spectral density of force and acceleration, frequency response function (FRF) of accelerance and the respective coherence.

3.5. Measurement points

The measurement points were distributed along the rod's largest dimension at positions with following distances from the beginning of the beam (the excited end):

- PA6 beam: 7.5 cm, 8.7 cm, 11.1 cm, 13.5 cm, 18.3 cm, 20.7 cm, 25.5 cm, 27.9 cm, 32.7 cm, 39.9 cm, 42.3 cm, 49.5 cm, 54.3 cm, 56.7 cm, 61.5 cm, 68.7 cm, 75.9 cm, 78.3 cm, 85.5 cm, 90.3 cm, 92.7 cm and 99.9 cm;

- PA6GF beam: 7.5 cm, 8.7 cm, 11.1 cm, 13.5 cm, 18.3 cm, 20.7 cm, 25.5 cm, 27.9 cm, 32.7 cm, 39.9 cm, 42.3 cm, 49.5 cm, 54.3 cm, 56.7 cm, 61.5 cm;
- PA3D beam: 7.5 cm, 8.7 cm, 11.1 cm, 13.5 cm, 18.3 cm, 20.7 cm, 25.5 cm, 27.9 cm;

The numbers of measurement points for PA6, PA6GF and PA3D beams are 22, 15 and 8, respectively. The distances are derived from the following sequence of prime numbers: 2, 3, 5, 7, 11, 13, 17, 19, 23, 29, 31, 37, 41, 43, 47, 53, 59, 61, 67, 71, 73 and 79. The proportionality of the distances to the prime numbers reduces (practically eliminates) the influence of the aliasing due to the finite length of the measurement points array.

4. RESULTS

For each of the polyamide beams, on the basis of the experimental results and applied correlation method with ANN approach to extension of frequency range, the following graphs have been created:

- a graph of the dispersion relationship between the wavenumber of a wave k and its frequency f,
- a comparison graph of the theoretical and experimental values for the resonant frequencies in the frequency range between 0 Hz to 6 kHz,
- a comparison graph of the theoretical and experimental values for the wavenumbers corresponding to the resonant frequencies in the frequency range between 0 Hz to 6 kHz,
- experimental values of wavenumbers corresponding to resonant frequencies in the frequency range between 0 Hz to 6 kHz for the purpose of visualization of values scattering around the line $k_m=(2m+1)\cdot k_0$ (theoretically these wavenumbers should lie on the line $k_m=(2m+1)\cdot k_0$).

Comparisons of theoretical and experimental values of fundamental frequency f_0, corresponding wavenumber k_0 and b_{kf} parameter ($b_{fk}=k/f^{1/2}$) are represented tabular for each of the polyamide beams. Theoretical values are calculated based on the values of density and Young’s modulus of elasticity obtained from the manufacturer's specification.

4.1. PA6 beam

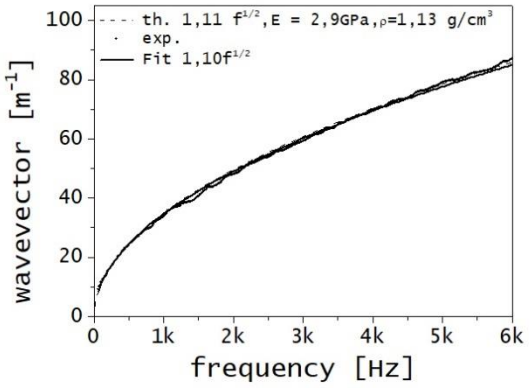

Figure 2: Dispersion relationship for PA6 beam

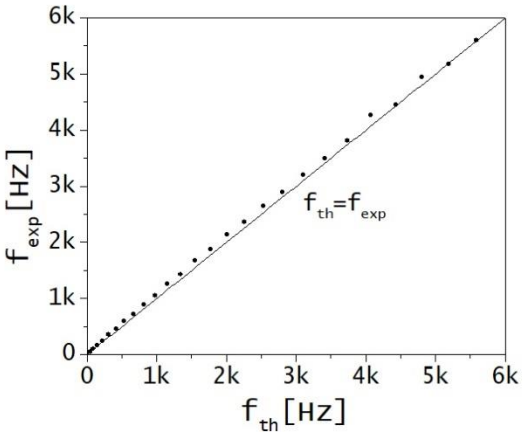

Figure 3: Comparison between theoretical and experimental values of resonant frequencies for PA6 beam

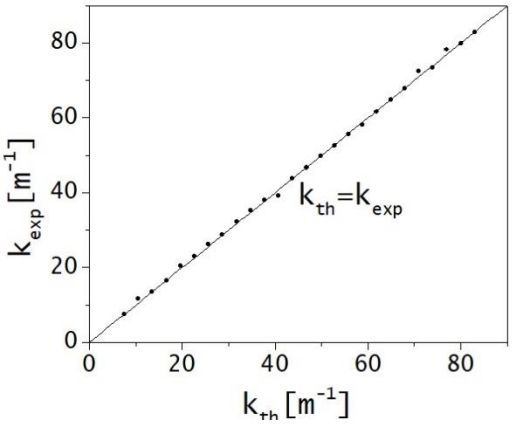

Figure 4: Comparison between theoretical and experimental values of wavenumbers corresponding to the resonant frequencies for PA6 beam

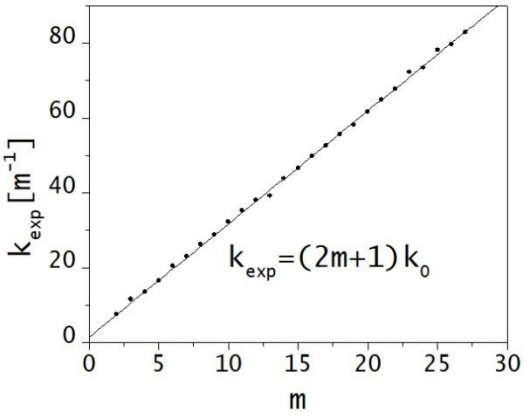

Figure 5: Experimental values of wavenumbers corresponding to resonant frequencies for PA6 beam

Table 2: Comparisons of theoretical and experimental values of f_0, k_0 and b_{kf} parameters for PA6 beam

	Theory	Experiment	Relative diff
k_0	1.51	1.52	1%
f_0	1.85	1.96	6%
b_{kf}	1.11	1.09	-2%

4.2. PA6GF beam

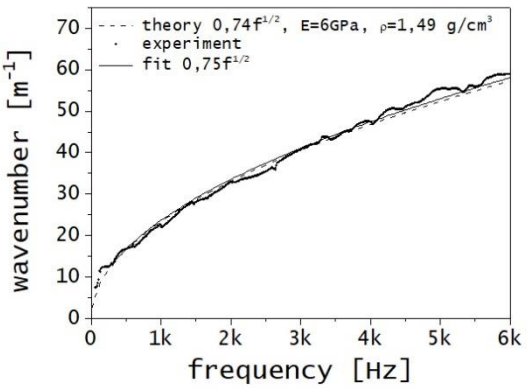

Figure 6: Dispersion relationship for PA6GF beam

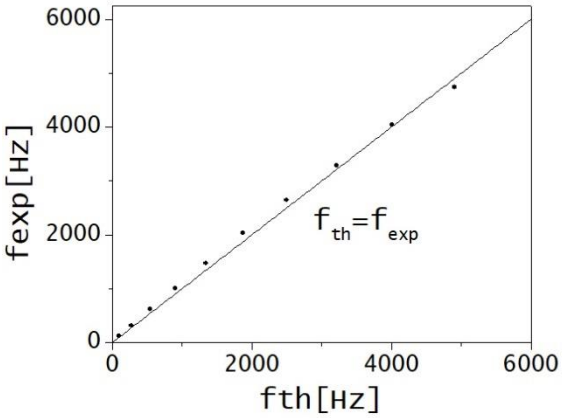

Figure 7: Comparison between theoretical and experimental values of resonant frequencies for PA6GF beam

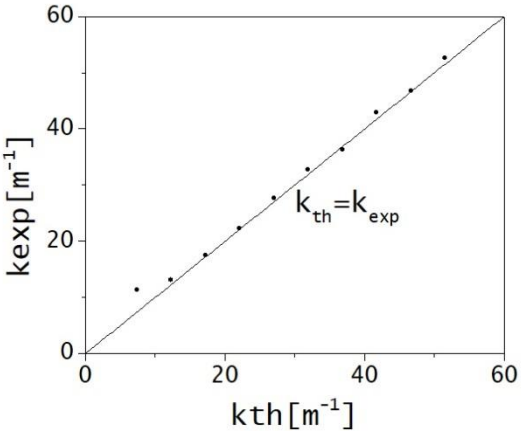

Figure 8: Comparison between theoretical and experimental values of wavenumbers corresponding to the resonant frequencies for PA6GF beam

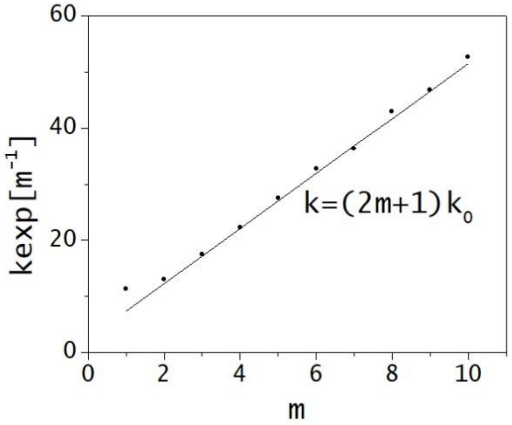

Figure 9: Experimental values of wavenumbers corresponding to resonant frequencies for PA6GF beam

Table 3: Comparisons of theoretical and experimental values of f_0, k_0 and b_{kf} parameters for PA6GF beam

	Theory	Experiment	Relative diff
k_0	5.24	5.15	-2%
f_0	11.12	11.80	6%
b_{kf}	0.74	0.73	-1%

4.3. PA3D beam

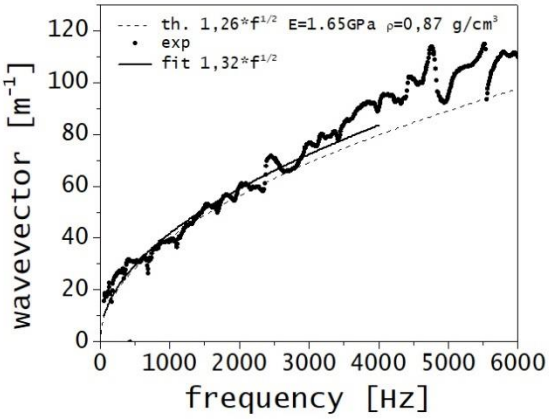

Figure 10: Dispersion relationship for PA3D beam

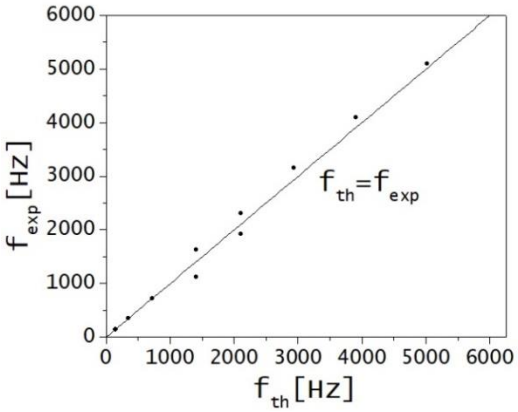

Figure 11: Comparison between theoretical and experimental values of resonant frequencies for PA3D beam

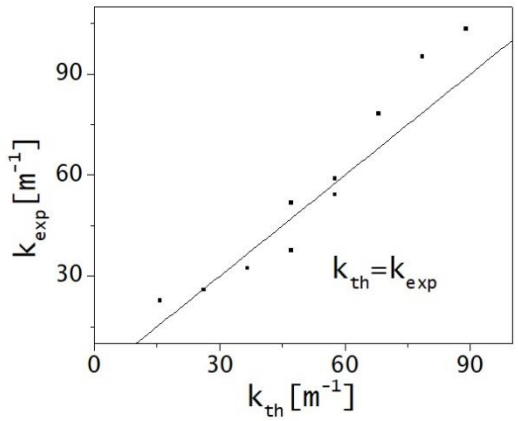

Figure 12: Comparison between theoretical and experimental values of wavenumbers corresponding to the resonant frequencies for PA3D beam

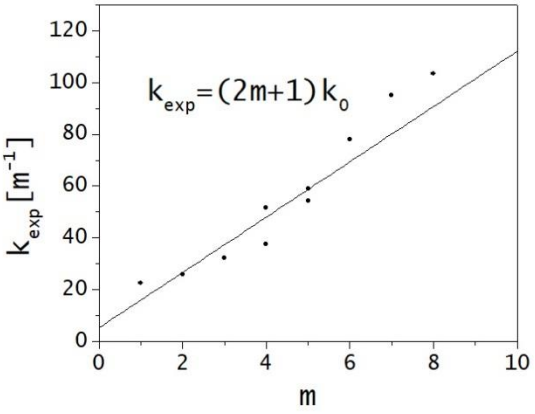

Figure 13: Experimental values of wavenumbers corresponding to resonant frequencies for PA3D beam

Table 4: Comparisons of theoretical and experimental values of f_0, k_0 and b_{kf} parameters for PA3D beam

	Theory	Experiment	Relative diff
k_0	5.24	5.15	-2%
f_0	17.38	17.04	-2%
b_{kf}	1.26	1.25	-1%

The obtained results show good agreement between the experimental and theoretical values for all three polyamide beams which were the objects of conducted analysis.

For the polyamide beam produced by selective laser sintering, slightly larger deviations between theoretical and experimental results (as shown in the Figures 10 to 13 and the Table 4) are due to the relatively short beam’s length compared to the lengths of the other two beams and, consequently, fewer measurement points and smaller amount of experimental data for the further analysis. Furthermore, the cross-sectional area of the rod produced by selective laser sintering is 1.5 and 4.6 times smaller than the cross-sectional areas of the other two polyamide rods cut from extruded plates, and, therefore, the mass of this rod is significantly smaller.

5. CONCLUSION

This paper presents a methodology for the experimental determination of the dispersion relationship of polyamide thin beams. The experiments were conducted on polyamide rods produced by cutting the extruded plates and polyamide rod produced by additive manufacturing (the process of selective laser sintering).

The obtained results show good agreement between the theoretical and experimentally obtained dispersion relationship for all three polyamide rods.

The slightly larger differences between theoretical and experimental values obtained for the rod made by selective laser sintering are due to its smaller dimensions and mass (compared to the dimensions and mass of rods produced by traditional cutting method), which directly affects the number of measurement points and measurement accuracy. Therefore, in further research, appropriate attention should be given to selecting dimensions and mass of the specimens.

ACKNOWLEDGEMENTS

The authors wish to express their gratitude to prof. Neil Fergusson from Institute of Sound and Vibration of University of Southampton for inspiration and support to this research effort.

The authors also wish to acknowledge the support of Ministry of Education, Science and Technology Development of Republic of Serbia through Grant 451-03-9/2021-14/200108.

REFERENCES

[1] Muhammad, A., Rahman, M. R., Baini, R., & Bakri, M. K. B. (2021). Applications of sustainable polymer composites in automobile and aerospace industry. In Advances in Sustainable Polymer Composites (pp. 185-207). Woodhead Publishing.

[2] Al-Lami, A., Hilmer, P., & Sinapius, M. (2018). Eco-efficiency assessment of manufacturing carbon fiber reinforced polymers (CFRP) in aerospace industry. Aerospace Science and Technology, 79, 669-678.

[3] Bodros, E., Pillin, I., Montrelay, N., & Baley, C. (2007). Could biopolymers reinforced by randomly scattered flax fibre be used in structural applications?. Composites Science and Technology, 67(3-4), 462-470.

[4] Toozandehjani, M., Kamarudin, N., Dashtizadeh, Z., Lim, E. Y., Gomes, A., & Gomes, C. (2018). Conventional and advanced composites in aerospace industry: Technologies revisited. Am. J. Aerosp. Eng, 5, 9-15.

[5] Palmer, R. J. (2001). Polyamides, Plastics. Encyclopaedia of Polymer Science and Technology. doi:10.1002/0471440264.pst251

[6] Beards, C. (1996). Structural vibration: analysis and damping. Elsevier.

[7] Rao, S.S. (2019). Vibration of continuous systems. John Wiley & Sons.

[8] Ferguson, N. S., Halkyard, C. R., Mace, B. R., & Heron, K. H. (2002). The estimation of wavenumbers in two-dimensional structures. Proceedings of ISMA2002: International Conference on Noise and Vibration Engineering, Leuven (Belgium), 799-806

[9] Maciejewski, M. W., Qui, H. Z., Rujan, I., Mobli, M., & Hoch, J. C. (2009). Nonuniform sampling and spectral aliasing. Journal of Magnetic Resonance, 199(1), 88-93.

[10] Tomić, J., Sinđelić, V., Ćirić Kostić, S., Bogojević, N., Šoškić, Z. (2021). Artificial neural network approach to extension of the frequency range for experimental determination of dispersion relationship using sparse spatial data. Acoustics and Vibration of Mechanical Structures. Timisoara (Romania)